Finite Element Analysis of Permeation Tests on Articular Cartilage under Different Testing Conditions Using COMSOL Multiphysics.

Grazia Spatafora[1*], Federica Boschetti[2]
[1,2] Structural Engineering Department, Politecnico di Milano, Milan, Italy, [2]IRCCS Istituto Ortopedico Galeazzi, Milan, Italy.
*Corresponding author: spatafora@stru.polimi.it

Abstract: Articular cartilage is composed of a charged solid matrix (proteoglycan and collagen fibres) and an interstitial fluid phase. The tissue is characterized by a very low permeability that guarantee the support and distribution of loads in diarthrodial joints and the transport of nutrients to chondrocytes. The permeability of articular cartilage decreases for increasing deformation of the solid matrix which occurs when a compression load is applied to the tissue. The study of permeability is very useful to understand the onset and progression of osteoarthritis and to regenerate cartilage by tissue engineering. Permeation studies in vitro are conceptually easy but practically difficult to be performed. In particular, it is not trivial to guarantee the sample seal while maintaining a uniform deformation. Furthermore, the measured variables are fluid pressure and flow through the sample, whereas it is not possible to measure the local strain, which otherwise can be evaluated by coupling computational studies of articular cartilage behaviour during permeation tests with experimental results. Using the poroelasticity module of COMSOL Multiphysics we performed various types of permeation tests varying the method used for positioning the sample in the test chamber (glued sample and o-ring on top) and the level of fluid pressure. To understand what is the better way to guarantee the sample seal, we evaluated the local strain, the deformed shape, the stress and the fluid pressure during the test and we compared these results with the ideal test ones.

Keywords: Articular Cartilage, Darcy's Law, Poroelasticity, Permeation Test.

1. Introduction

Articular cartilage is composed of a charged solid matrix phase (proteoglycan macromolecules and collagen fibres), an interstitial fluid phase, and an ion phase (Mow et al, 1999). The function of articular cartilage is to support and distribute loads in the diarthrodial joints, to minimize friction between articular surfaces by the maintenance of a lubricating fluid film (Mow and Setton 1998) and to transport nutrients to cells.

Experimental investigation of cartilage biomechanics during compression is typically performed by using confined or unconfined compression tests, or indentation. The equilibrium response of articular cartilage is satisfactorily described, for small deformations, by the homogeneous isotropic elastic model (Hayes et al, 1972). In particular, unconfined and confined compression tests are commonly used to evaluate the Young's modulus (E) and the aggregate modulus (H_A), respectively.

Mow et al. (1980) introduced the apparent permeability (k) as a parameter regulating the velocity of fluid exudation from the tissue. Due to the compaction of the solid matrix during compression, the permeability of articular cartilage is not a constant property of the tissue; in fact, it decreases for increasing deformation (Mansour and Mow, 1976), according to an exponential curve (Lai and Mow, 1980). It also varies through the depth of the tissue as other mechanical properties.

Progression of osteoarthritis and cartilage regeneration are two phenomena connected with the permeability of the tissue. A constant value of permeability (apparent permeability) can be identified by models of confined compression (Kwan et al, 1984), or indentation tests (Mow et al, 1989), whereas to study the relationship between matrix deformation and permeability more complex models or direct measurements (Boschetti et al, 2006, Heneghan and Riches, 2008, Reynaud and Quinn, 2006) are needed. Permeation studies in vitro are conceptually easy but practically difficult to be performed. In particular, it is not trivial to guarantee the sample seal while maintaining a uniform deformation. Furthermore, the measured variables are fluid pressure and flow through the sample, whereas it is not possible to measure the local strain, which otherwise can be evaluated by coupling computational studies of articular cartilage behaviour during permeation test with experimental results. We therefore performed numerical simulations, based on the poroelasticity theory, of permeation tests varying

the method used for positioning the sample into the test chamber. For each design we evaluated the local strain distribution which is essential to a precise calculation of the permeability from experimental tests.

2. Poroelasticity and Darcy's Law

Poroelastic theory describes articular cartilage composed by a porous-permeable solid matrix saturated with interstitial fluid according to the biphasic model.

The stress-strain-pore pressure constitutive relation for a saturated porous medium linearly relates the total stress $\boldsymbol{\sigma}$ to strain $\boldsymbol{\varepsilon}$ and to the pressure fluid p (e1):

$$\boldsymbol{\sigma_{total}} = \boldsymbol{C\varepsilon} - \alpha p\boldsymbol{I} \quad \text{(e1)}$$

where $\boldsymbol{C}$ is the anisotropic drained elasticity tensor and α is called Biot-Willis coefficient that relates the volume of fluid expelled to the volumetric change of the medium. The sample is considered incompressible and isotropic, so the Biot-Willis coefficient is $\alpha = 1$.

The total stress is composed by two components: the Cauchy component on the solid matrix and the fluid pressure (e2,e3,e4).

$$\boldsymbol{\sigma_{total}} = \boldsymbol{\sigma_{fluid}} + \boldsymbol{\sigma_{solid}} \quad \text{(e2)}$$
$$\boldsymbol{\sigma_{solid}} = -\phi^s p\boldsymbol{I} + \boldsymbol{C\varepsilon} \quad \text{(e3)}$$
$$\boldsymbol{\sigma_{fluid}} = -\phi^f p\boldsymbol{I} \quad \text{(e4)}$$

Where ϕ^f is the volume fraction of the fluid that is equal to porosity because the medium is saturated (e5):

$$\phi^f = \frac{V^f}{V^{total}} \quad \text{(e6)}$$

And

$$\phi^s = 1 - \phi^f. \quad \text{(e7)}$$

They are supposed constant during the permeability test.

We assumed that the porous medium is isotropic, so e8 is:

$$\boldsymbol{\sigma_{solid}} = -\phi^s p\boldsymbol{I} + \lambda_s tr(\varepsilon)\boldsymbol{I} + 2\mu_s\boldsymbol{\varepsilon} \quad \text{(e8)}$$

where λ_s and μ_s are Lamé constants.

The continuity equations for two incompressible phases are (e9,e10):

$$\frac{\partial \phi^s}{\partial t} + \nabla(\phi^s v^s) = 0 \quad \text{(e9)}$$
$$\frac{\partial \phi^f}{\partial t} + \nabla(\phi^f v^f) = 0 \quad \text{(e10)}$$

And the momentum equations are (e11,e12):

$$\rho^s \frac{Dv^s}{Dt} = \nabla\sigma^s + \pi^s + b^s \quad \text{(e11)}$$
$$\rho^f \frac{Dv^f}{Dt} = \nabla\sigma^f + \pi^f + b^f \quad \text{(e12)}$$

Where $\frac{Dv^i}{Dt}$ is the material derivative relative to the i[th] phase, π^i is the diffusive drag and it comes from the locally produced force on the i[th] phase resulting from its interaction with the other constituent and b^i is a body force. We assume that there are no external body forces and that inertia can be neglected . It comes from the relatively large diffusive drag due to the extremely low permeability of these tissues when compared with the inertia forces (e13,e14,e15):

$$\nabla\sigma^s + \pi^s = 0 \quad \text{(e13)}$$
$$\nabla\sigma^f + \pi^f = 0 \quad \text{(e14)}$$
$$\pi^s = L(v^s - v^f) = -\pi^f \quad \text{(e15)}$$

Where L is called diffusive drag coefficient that is related to porosity and permeability, $v^s = \frac{\partial u^s}{\partial t}$ and v^f is calculated from the Darcy's law (e16):

$$\rho^f \cdot \boldsymbol{v^f} = -\boldsymbol{H} \cdot \nabla p \quad \text{(e16)}$$

The matrix $\boldsymbol{H}$ represents the porous medium hydraulic resistance and is (e17):

$$\boldsymbol{H} = \frac{\rho^f \boldsymbol{K}}{\phi^f \eta} \quad \text{(e17)}$$

Where η is the fluid viscosity and $\boldsymbol{K}$ is the tensor of the apparent permeability that in our case is a scalar k because we consider an isotropic solid matrix. So, e16 is (e18):

$$q = \phi^f v^f = -\frac{k}{\eta}\nabla p \quad \text{(e18)}$$

The above equation allow to completely describe the stress and deformation variables that characterize the mechanical behavior of articular cartilage.

3. The Permeation Test

The permeation test gives a direct measurement of the apparent permeability *k*.

The figure below (f1) is a schematic representation of a typical permeation test:

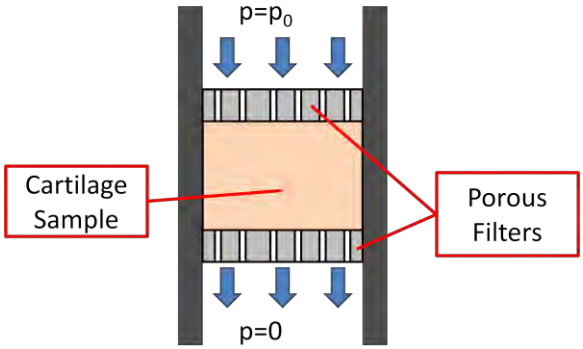

Figure 1. Schematic representation of permeation test.

The sample is supported by two rigid porous filters. A fluid pressure is applied on top of the sample, and flow through the sample is measured. The apparent permeability is then evaluated by applying the Darcy's law. Other devices permit the imposition of flow and the measurement of the pressure (Périé et al., 2005; Reynaud et al., 2006; Heneghan et al., 2006).

If the test is not perfectly confined, fluid will pass around the sample instead through it (f2).

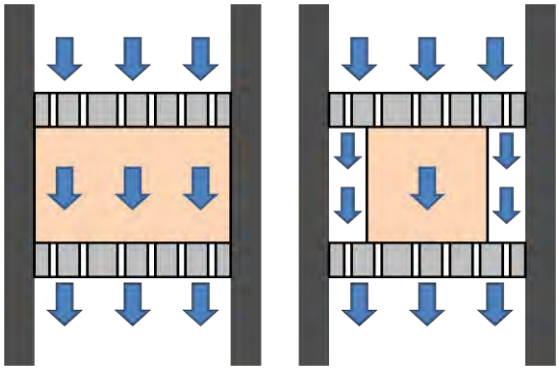

Figure 2. Difference between a perfectly confined test and a not one.

This problem introduces a false measurement of the apparent permeability of the sample.

The aim of this work is the evaluation of two different methods to confine the sample:

- The outer edges of the sample are glued to the device;
- An o-ring is used to clamp the sample outer edges to impose the passage of the fluid through the center of the sample.

Choosing the method to seal the sample is a crucial point for the design of a device that permits the measurement of apparent permeability.

4. Use of COMSOL Multiphysics

Soils and cartilage have an analogous mechanical behavior, so we used the *Poroelasticity* model built inside the COMSOL Multiphysics *Earth Science Module* to simulate the permeation test. In this module there is a model called *Poroelasticity* that implements the biphasic model.

4.1 Geometry

Samples used during in vitro permeation tests are typically of cylindrical shape with thickness between 0.5 and 2 mm and diameter between 5 and 12 mm. The maximum sample thickness is limited by the tissue thickness, the maximum diameter by the need of a flat surface.

In our simulations we considered a diameter of 12 mm and a thickness of 1 mm.

So, the geometry can be modeled as axial-symmetry (f3).

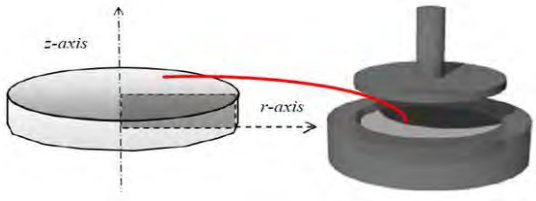

Figure 3. Geometry and symmetry used in simulations.

4.2 Subdomain Settings

The COMSOL Multiphysics Material library does not contain articular cartilage, so we created a new material and we considered water as the fluid phase. The cartilage was described as a multiphase material

constituted of an incompressible, isotropic, linear, elastic solid phase, and an incompressible fluid phase (Mow et al, 1980). The model parameters were Young's modulus (E), Poisson's ratio (ν), hydraulic permeability (k) and porosity (Φ). E, ν, k and Φ were set to 0.5 MPa, 0.25, 10^{-18} m^2, and 0.75 respectively (Boschetti et al., 2006).

4.3 Boundary settings

The aim of our simulation is to understand which is the better way, between glue and o-ring, to seal the cartilage sample inside the permeation test device. At first, we simulated an ideal permeation test to have a reference model to compare the glue and o-ring model results to.

The boundary conditions (BCs) used in the three different tests are resumed in the following figure (f5).

For every simulation we imposed a loading pressure ramp for 50s (t_1) and a costant load for 5000s from 0 to 10 atm with a step of 1 atm and from 0 to 100 atm with a step of 10 atm.

4.4 Mesh

We used quad elements for the mesh, which are proper for simple geometry without holes. In particular the implemented elements, using a mapped mesh presented in COMSOL, are *lagrangian-quadratic*.

5. Results an Discussion

The software can display the effective load on the cartilage sample. The effective load remains constant despite a linear variation of fluid pressure (f4) for $t \geq t_1$ (end of load ramp).

The results in terms of pressure and deformation in the three different conditions of the permeation tests evidence how both the glued sample and the o-ring one present a large central zone in which the mechanical behavior is analogous to the ideal test simulation (f6).

6. Conclusions

The comparison between the effective load on the cartilage and the fluid pressure underlines how the load is transferred from the fluid to the solid phase and permits validation of the model used (f4).

COMSOL simulations permit to understand as both glued and o-ring solution are good possibilities to guarantee fluid flow only through the sample (f6). For practical reasons, the o-ring solution should be the preferred choice, because glue is difficult to use. a small glue quantity may cause water to seep through the edges of the sample, on the contrary a large glue quantity may clog the tiny cartilage pores.

The choice of the constraint on the sample allowed us to design a device to measure the permeability of articular cartilage. The set up allows both to test cartilage as described above that through the introduction of an initial note deformation on the specimen to obtain values of intrinsic permeability (Mow et al., 1989).

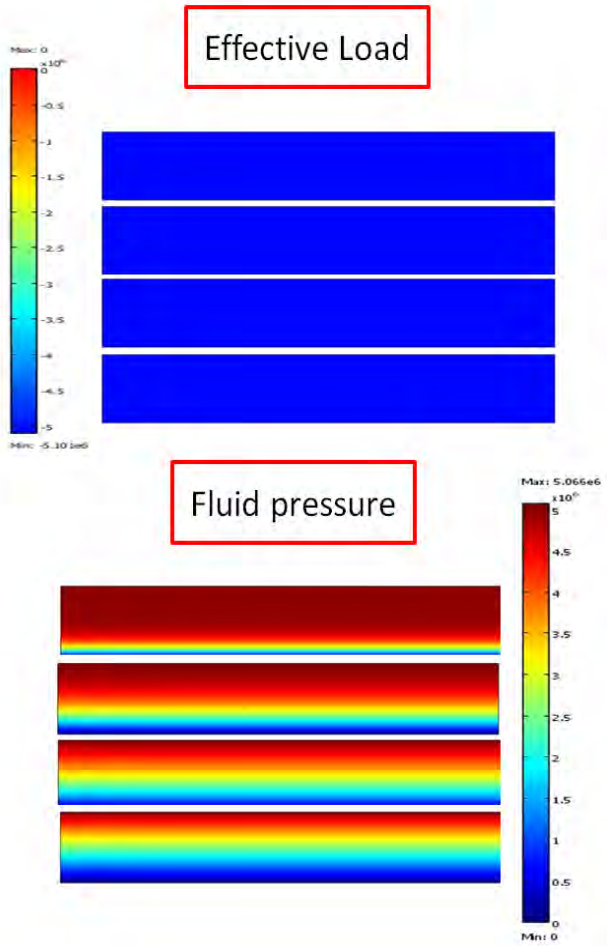

Figure 4. Comparision between the effective stress and fluid pressure

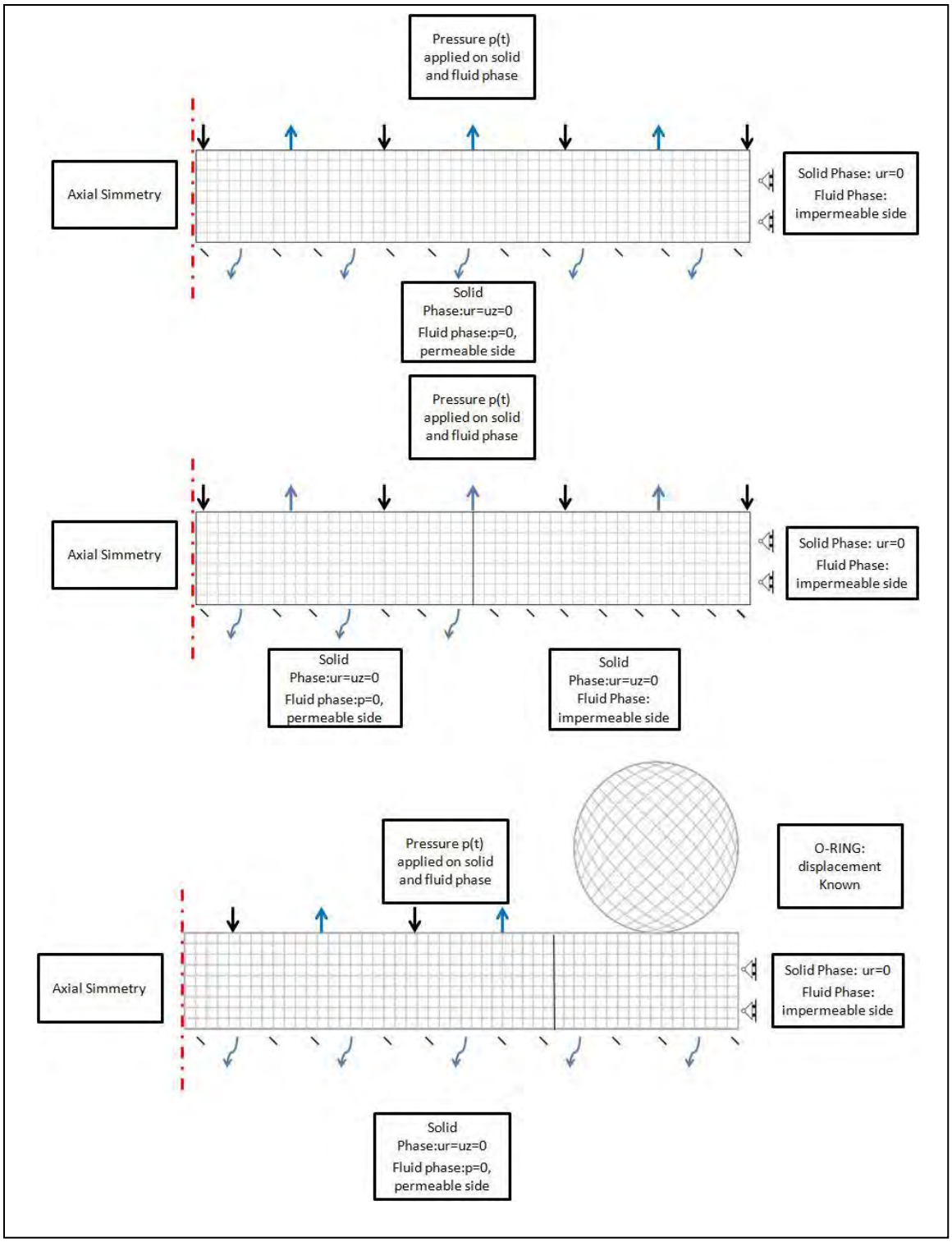

Figure 5. BCs used in the three different tests.

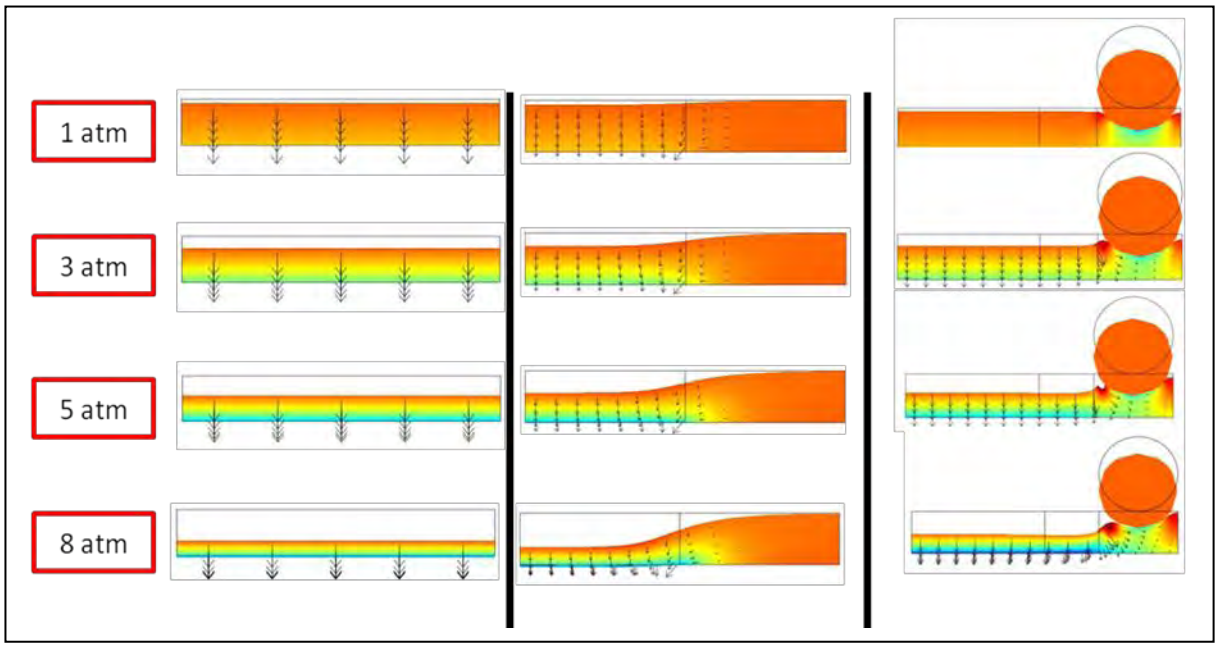

Figure 6. Strain results for different pressures.

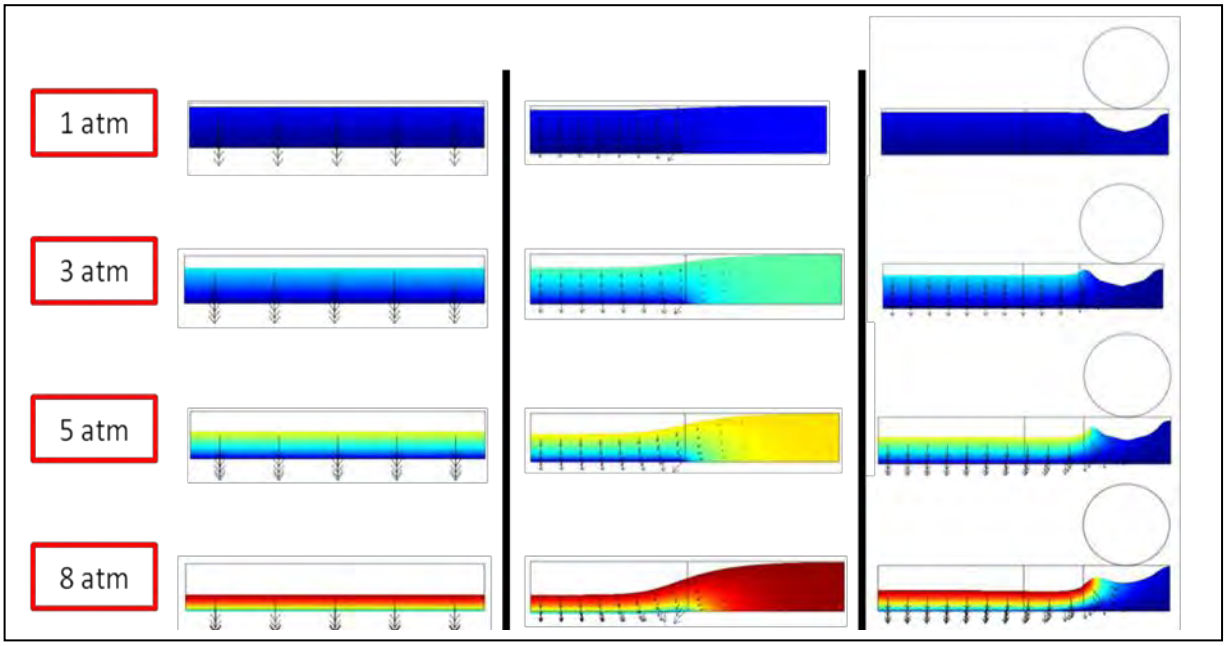

Figure 7. Fluid pressure results

7. References

1. Boschetti F, Gervaso F, Pennati G, Peretti GM, Vena P, Dubini G. Poroelastic numerical modelling of natural and engineered cartilage based on in vitro tests, *Biorheology* **43**, 235–247 (2006).

2. Hayes WC, Keer LM, Herrmann G, Mockros LF, A mathematical analysis for indentation tests of articular cartilage, *Journal of Biomechanics*, **5**, 541-551 (1972).

3. Heneghan P, Riches ER Determination of the strain-dependent hydraulic permeability of compressed bovine nucleus pulposus, *Journal of Biomechanics* **41**, 903-906 (2006).

4. Kwan MK, Lai WM, Mow VC, Fundamentals of fluid transport through cartilage in compression, *Ann. Biomed. Eng.* **12**, 537-58 (1984).

5. Mow VC, Kwei SC, Lai WM, Armstrong CG, Biphasic creep and stress relaxation of articular cartilage in compression: theory and experiments, *Journal of Biomechanics*, Eng. **102**, 73-84 (1980).

6. Mow VC, Gibbs MC, Lai WM, Zhu WB, Athanasiou KA, Biphasic indentation of articular cartilage-II. A numerical algorithm and an experimental study, *Journal of Biomechanics*, **22**, 853-861 (1989).

7. Mow VC, Setton LA, Mechanical properties of normal and osteoarthritic articular cartilage, in: *Osteoarthritis*, K.D. Brandt, M. Doherty and L.S. Lohmander, eds, Oxford Uni-versity Press, Oxford, UK, 108-122 (1998).

8. Mow VC, Wang CC Hung CT, The extracellular matrix, interstitial fluid and ions as a mechanical signal transducer in articular cartilage, *Osteoarth. Cartil.*, **7**, 41-58 (1999).

9. Périé D, Korda D, Iatridis JC Confined compression experiments on bovine nucleus pulposus and annulus fibrosus: sensitivity of the experiment in the determination of compressive modulus and hydraulic permeability. *J Biomech*, **38(11)**, 2164-71 (2005).

10. Reynaud B, Quinn TM, Anisotropic hydraulic permeability in compressed articular cartilage. *Journal of Biomechanics*, **39**, 131-137 (2006).